Elucidation of cGMP-Dependent Induction of Mitochondrial Biogenesis Through Protein Kinase G and p38 MAPK in the Kidney

Pallavi Bhargava[1]*, Jaroslav Janda[1]*, and Rick G. Schnellmann[1,2]

* These authors contributed equally to this work

[1]*Department o Pharmacology and Toxicology, College of Pharmacy, University of Arizona, Tucson, Arizona;* [2]*Southern Arizona Veterans Affairs Health Care System, Tucson, Arizona*

Running Title: cGMP Induced Mitochondrial Biogenesis in the Kidney

Corresponding Author: Dr. Rick G. Schnellmann, PhD
University of Arizona
Department of Pharmacology and Toxicology
College of Pharmacy
Roy P. Drachman Hall, Rm. B307B
1295 N. Martin Ave
Tucson, AZ 85721
schnell@pharmacy.arizona.edu
520-626-1657

Abstract

Previous studies have shown that cGMP increases mitochondrial biogenesis (MB). Our laboratory has determined that formoterol and LY344864, agonists of the β_2-adrenergic and 5-HT_{1F} receptor, respectively, signal MB in a sGC-dependent manner. However, the pathway between cGMP and MB produced by these pharmacological agents in renal proximal tubule cells (RPTC) and the kidney, has not been determined. We show that treatment of RPTC with formoterol, LY344864, or riociguat, an sGC stimulator, induces MB through protein kinase G (PKG), a target of cGMP, and p38, an associated downstream target of PKG and a regulator of PGC-1α expression in RPTC. We also examined if p38 plays a role in PGC-1α phosphorylation *in vivo*. L-Skepinone, a potent and specific inhibitor of p38α and p38β administration to naïve mice inhibited phosphorylated PGC-1α localization in the nuclear fraction of the renal cortex. Taken together, we have demonstrated a pathway, sGC/cGMP/PKG/p38/PGC-1α, for pharmacological induction of MB and the importance of p38 in this pathway.

Introduction

In the presence of nitric oxide (NO), soluble guanylyl cyclase (sGC) produces cGMP from GTP. The resulting cGMP can bind to cGMP gated ion channels, phosphodiesterases, and protein kinase G (PKG)[9]. As such, cGMP plays a role in a variety of processes in the cell including mitochondrial biogenesis (MB)[21,22].

PKG is a serine/threonine kinase that exists in two forms, PKG1 and PKG2[14]. In renal tubular cells, PKG1 activity and expression decreased when exposed to cisplatin[19]. Increasing PKG1 activity protected mitochondrial function and prevented cell apoptosis[19]. In brown adipose tissue, natriuretic peptides activate GC resulting in activated PKG[1,5] and the induction of MB[12]. Adipocytes exposed lipoamide also undergo MB through PKG[28].

Activated PKG leads to the phosphorylation of p38 in human adipocytes when stimulated with naturetic peptides[1,13]. Browning et al., showed the importance of activated PKG in NO-induced p38 phosphorylation in 293T fibroblasts[3]. It was also shown in human platelets stimulated by thrombin, that p38 activation is necessary for integrin activation and activated PKG plays an important role in this mechanism[18]. These studies show that activated PKG plays a role in activating p38 in certain cell types.

PGC-1α is thought to be the master regulator of MB[15,25]. Phosphorylated p38 can directly phosphorylate PGC-1α at three sites: Threonine 298, Threonine 262, and Serine 265[8]. Phosphorylation at these sites can increase the stability of PGC-1α, promote its translocation into

the nucleus and induce transcription of PGC-1α target genes[12]. Puigserver et al, showed that cultured muscle cells treated with LPS resulted in p38-mediated PGC-1α phosphorylation[24].

Our laboratory showed that maximal mitochondrial respiration (i.e. uncoupled respiration), a marker of MB, increases in renal proximal tubule cells (RPTC) treated with the membrane soluble cGMP analogue 8-Br-cGMP but not 8-Br-cAMP, suggesting that cGMP is responsible for inducing MB rather than cAMP in RPTC[31]. Moreover, we have shown that cGMP is a key player in inducing MB by two G-protein-coupled receptor (GPCR) agonists. Formoterol, a β_2 adrenergic receptor (β_2AR) agonist, and LY344864, a 5-HT_{1F} receptor agonist, induced MB through the $G_{\beta/\gamma}$ subunit, Akt, sGC, and cGMP[4,10]. Our studies are consistent with reports for other GPCRs, such as cannabinoid type 1 receptor, inducing MB through increased NO production[30].

However, the pathway from cGMP to MB following pharmacological stimulation in highly oxidative renal epithelial cells is not clear. We propose that formoterol, LY344864, and riociguat, an sGC stimulator that increases cGMP, activates protein kinase G (PKG), which leads to the phosphorylation of p38. In turn, p38 phosphorylates PGC-1α to facilitate translocation to the nucleus and produce MB.

Material and Methods

Reagents:

L-Skepinone was purchased from Selleckchem (Houston, TX). LY344864 and KT5823 was purchased from Tocris (Minneapolis, MN). Riociguat was purchased from Biovision (Milpitas, CA). Formoterol fumarate was purchased from Sigma (St. Louis, MO).

In vitro Studies:

Renal Proximal tubule cells (RPTC) were isolated from female NZW rabbit (2kg) kidneys using the iron oxide perfusion method[23]. Cells were plated and grown on 35 mm tissue culture dishes in conditions that are similar to physiological conditions *in vivo*. Confluent RPTC were treated with riociguat (10 μM), LY344864 (10 nM), formoterol (30 nM) or vehicle, consisting of DMSO (<0.5%). For the inhibitor studies, RPTC were pretreated with 100 nM KT5823 (KT) or 100 nM skepinone (SK) for 30 min. Riociguat, formoterol, LY344864, or DMSO was added to RPTC, incubated for 2 hr and harvested for further analysis. The concentrations of formoterol and LY344864 have previously be shown to induce MB in RPTC[4,10].

In vivo Studies:

Skepinone was dissolved in DMSO and diluted in sterile saline. Final DMSO concentration was 2%. Eight to nine-week old male C57BL/6 mice (20–25 g from Charles River Laboratories) were injected intraperitoneally with skepinone at 1, 3, or 10 mg/kg or vehicle. After 6 hr the mice were euthanized and kidneys were removed. Part of the kidney was flash frozen or processed for subcellular fractionation. Animal studies and animal use was approved by the Institutional Animal Care and Use Committee at the University of Arizona.

Subcellular Fractionation:

RPTC were harvested in sucrose isolation buffer containing 250 mM sucrose, 1 mM EGTA, 10 mM HEPES, and 1 mg/ml fatty acid free BSA at a pH of 7.4. Cells were homogenized using a dounce homogenizer and centrifuged at 700 g for 5 min. The cytosolic supernatant was stored in phosphatase inhibitors (1:100), 1mM sodium orthovanadate, and 1 mM sodium fluoride, and Triton X-100 and SDS at 4%. The pellet was washed twice in isolation buffer and centrifuged at 1,000 g for 5 min. The pellet/nuclear fraction, was resuspended in RIPA buffer containing 50 mM Tris-HCl, 150 mM NaCl, 0.1% SDS, 0.5% sodium deoxycholate, 1% Triton X-100, pH 7.4 with phosphatase inhibitors (1:100), 1mM sodium orthovanadate, and 1 mM sodium fluoride. Purity of the cytosolic and nuclear fractions was determined using immunoblot analysis. Histone H3 and/or lamin B1 were used as nuclear markers, and α-tubulin was used as a cytosolic marker. Antibodies for Histone H3 were purchased from Cell Signaling Technology (Danvers, MA). Antibodies for lamin B1 and α-tubulin were purchased from Abcam (Cambridge, MA).

Immunoblot Analysis

RPTC or snapped frozen mouse kidney cortex was added to RIPA buffer. Cells were sonicated for approximately 10 seconds and centrifuged at 7,500 g for 5 min at 4°C. Supernatants were removed and protein was measured using a BCA assay. Equal protein was loaded onto 4-15% SDS page gels and separated by gel electrophoresis. Protein was transferred onto nitrocellulose membranes and blocked in 5% milk or 5% bovine serum albumin dissolved in TBST. Membranes were incubated with primary antibodies overnight. Membranes were washed in TBST 3 times for 5 min, incubated with a horseradish peroxidase–conjugated secondary

antibody, and visualized using enhanced chemiluminescence (Thermo Scientific) and GE ImageQuant LAS4000 (GE Life Sciences). Optical density was determined using the ImageJ software from NIH. Primary antibodies p-vasodilator-stimulated phosphoprotein (VASP) Ser239 (1:1,000), phospho-p38 MAPK (Thr180/Tyr182) (1:1000), and p38 MAPK (1:1000) were purchased from Cell Signaling Technology (Danvers, MA).

Immunoprecipitation

Dynabeads™ Protein G Immunoprecipitation Kit (Thermofisher) was used to immunoprecipitate PGC-1α in the cytosolic and nuclear fractions. Protein (200 μg) from cytosolic and nuclear fractions were precleared with Pierce Protein A/G Plus Agarose beads (Thermofisher) for 2 hr and then centrifuged at 14,000g for 10 min at 4°C. Dynabeads™ magnetic beads were incubated with 10 μg of PGC-1α antibody for 4 hr at room temperature. Supernatants from the precleared cytosolic and nuclear fractions were added to the magnetic beads and PGC-1α antibody and incubated with rotation overnight at 4° C. PGC-1α was immunoprecipitated and eluted (denaturing elution) based on manufacturer's instructions. The resulting supernatant was directly loaded on to a 4-15% SDS page gel and separated by gel electrophoresis. After protein transfer, one nitrocellulose membrane was blocked in 5% milk for measuring total PGC-1α and the other was blocked in 5% bovine serum albumin for measuring phosphorylated serine/threonine residues for 1 hr. Membranes were incubated with phosphoserine/threonine (1:1,000) antibody from Abcam (Cambridge, MA) or PGC-1α antibody (1:1,000) from EMD Millipore (Billerica, MA) overnight at 4°C. After the membranes were washed in TBST 3 times, they were incubated in horseradish peroxidase-conjugated secondary antibodies from Abcam (Cambridge, MA) for 2 hrs at room temperature. Membranes were visualized as described above.

Statistics

Data are represented as mean ± SEM. RPTC isolated from a single rabbit represent N=1. For a single comparison, Student's *t*-test was performed. Multiple comparisons were subjected to one-way ANOVA and Tukey's post hoc test with $p<0.05$ being statistically significant between means. Statistical differences between means are denoted by an *, #, or $ accordingly.

Results

Riociguat activates PKG and is blocked by KT5823

To elucidate the signaling pathway from sGC to nuclear PGC-1α phosphorylation, RPTC were treated with riociguat (10μM), a sGC stimulator that targets the reduced form of sGC[2,16,20,29]. The reduced form of sGC predominates in naïve cell types and increases cGMP directly. cGMP production can activate PKG, and PKG activation was determined by measuring the phosphorylation of vasodilator-stimulated phosphoprotein (VASP) at site serine 239, a specific target of PKG[6].

RPTC were treated with riociguat for 2 hr, resulting in a 1.3-fold increase in VASP phosphorylation compared to controls (Figure 1). Pretreatment of KT5823, a PKG inhibitor, for 30 min and subsequent treatment with vehicle or riociguat for 2 hr resulted in a decrease in VASP phosphorylation to control levels, demonstrating that KT inhibits PKG. Pretreatment with KT5823 alone lowered phosphorylation of VASP in RPTC to below control levels.

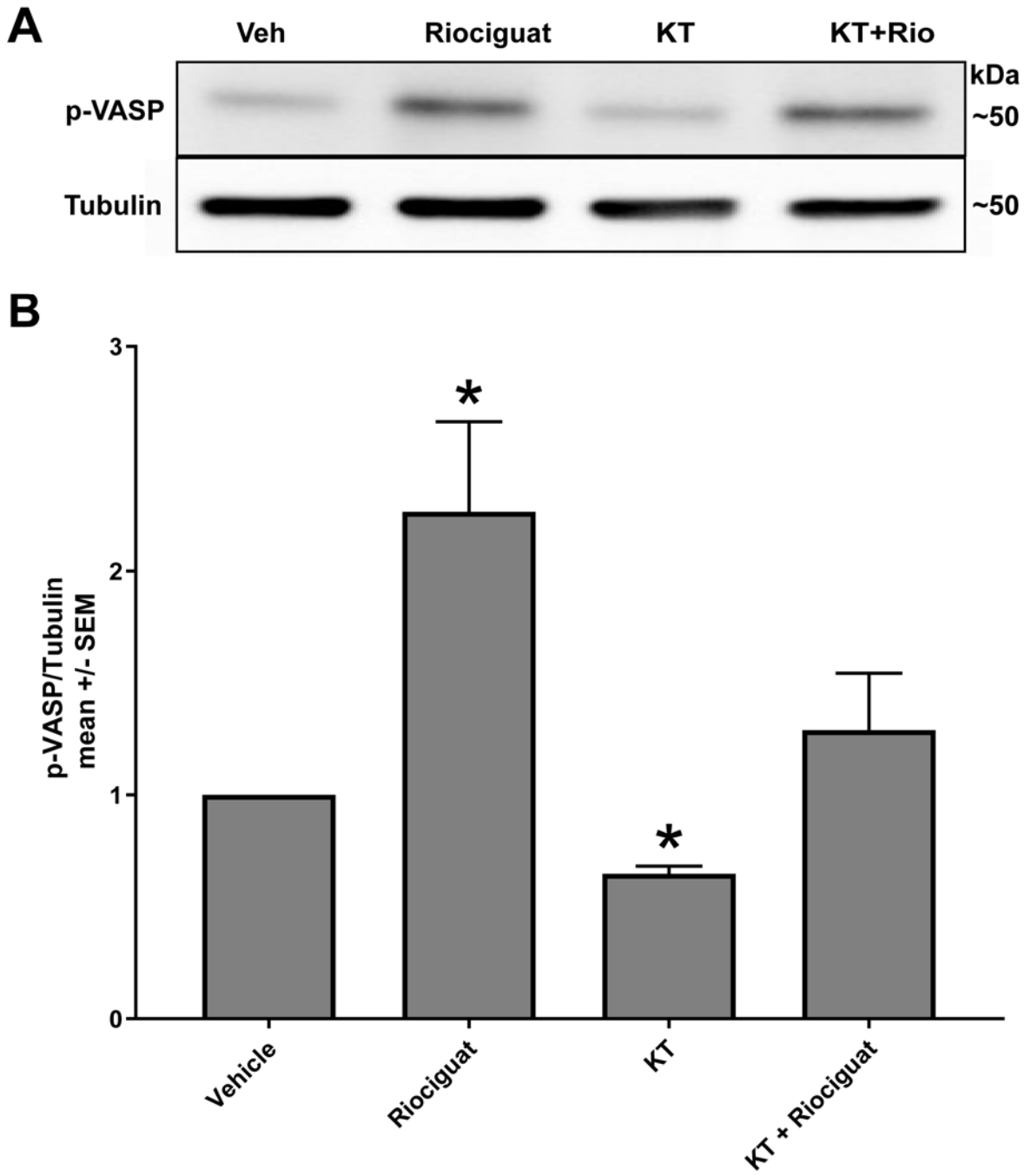

Figure 1: Riociguat phosphorylates VASP (p-VASP) and is blocked by KT5823 (KT)
A) Representative immunoblot for p-VASP and tubulin after treatment. B) Densitometry analysis for p-VASP protein. Data are represented as mean S.E., N=6-7. * represents significance compared to Vehicle ($p<0.05$).

Riociguat activates p38 through PKG

We hypothesized that p38 is the mediator between PKG activation and PGC-1α phosphorylation in RPTC. Riociguat treated RPTC increased p-p38 2.1-fold at 2 h. Pretreatment with KT5823 for 30 min with subsequent treatment with vehicle or riociguat for 2 hr resulted in a decrease in p-p38 to control levels (Figure 2A-2B).

To validate skepinone inhibition of p38 phosphorylation at 2 h in the presence and absence of riociguat, RPTC were treated with skepinone for 30 min and then treated with vehicle or riociguat for 2 h. Skepinone inhibited p-p38 when RPTC were treated with riociguat (90%) or vehicle (80%) at 2 h (Figure 2C-D).

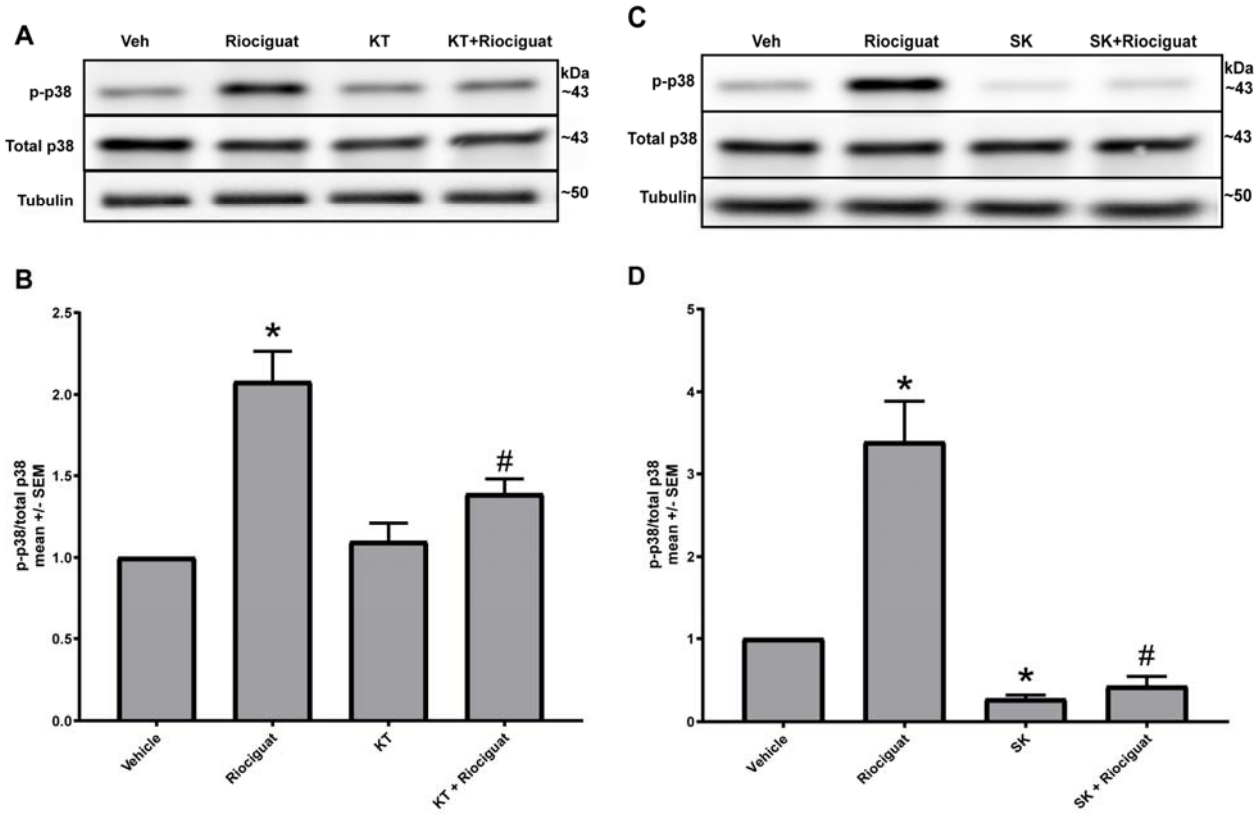

Figure 2: KT5823 and skepinone inhibit phosphorylation of p38

A and C) Representative blot for p-p38, total p38, and tubulin after treatment. B and D) Densitometry analysis for p-p38 protein. Data are represented as mean S.E., N=6-7. * represents significance compared to Vehicle ($p<0.05$). # represents significance compared to riociguat ($p<0.05$).

LY344864 and formoterol activate p38

Based on the above results, we examined if p38 plays a role in the signaling pathways of formoterol and LY344864. We treated RPTC with vehicle, formoterol, or LY344864 for 2 hr. p38 phosphorylation increased 1.6-fold and 1.9-fold when exposed to formoterol and LY344864, respectively (Figure 3). RPTC were pretreated with skepinone for 30 min and exposed to vehicle, formoterol, and LY344864 for 2 h. Skepinone alone inhibited p-p38 by 70% compared to vehicle control. Skepinone pretreatment inhibited p-p38 by 80% after formoterol and LY344864 treatment.

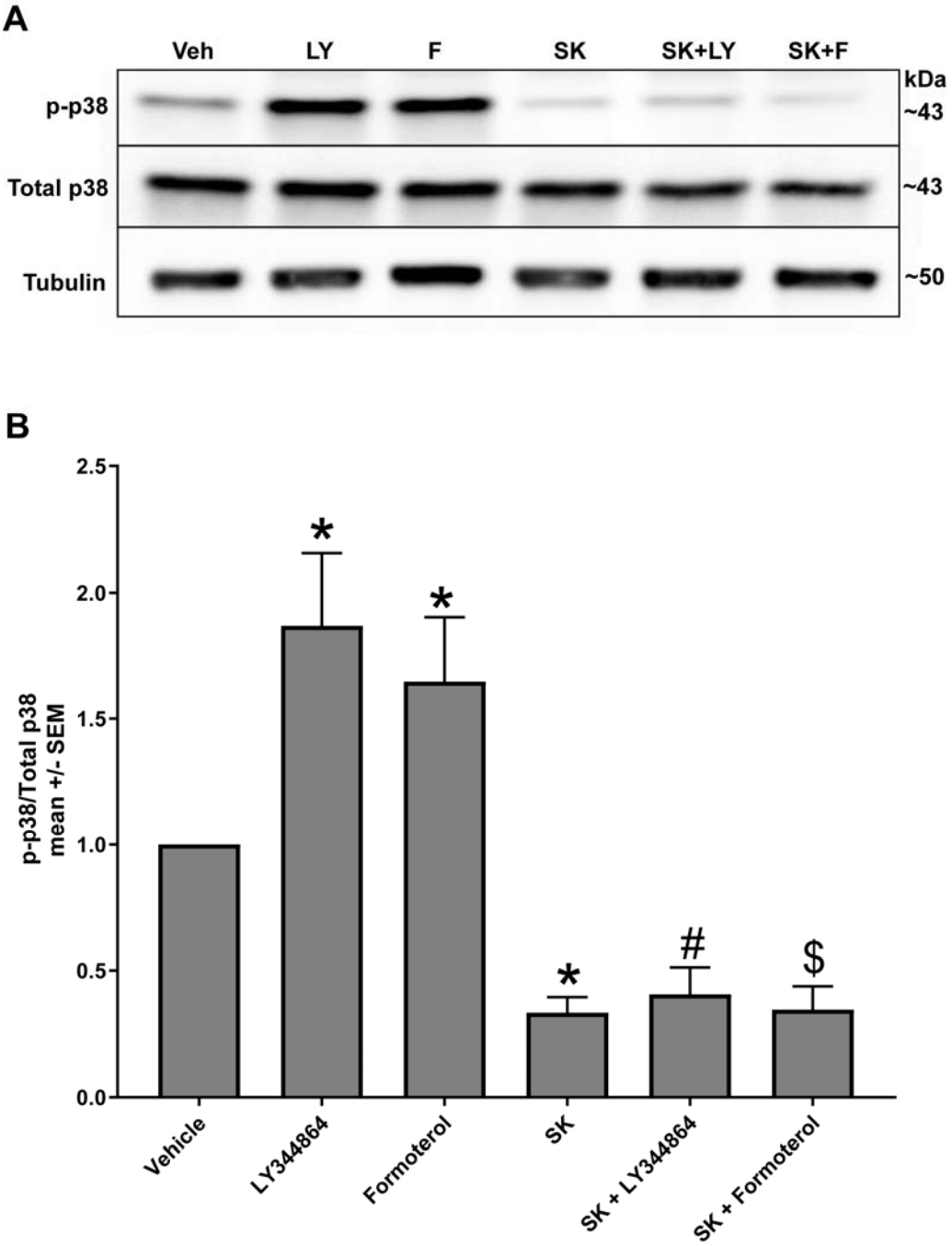

Figure 3: Skepinone inhibits LY344864 and formoterol mediated p38 phosphorylation
A) Representative blot for p-p38, total p38, and tubulin after treatment. B) Densitometry analysis for p-p38 protein. Data are represented as mean S.E., N=8. * represents significance compared to Vehicle ($p<0.05$). # represents significance compared to LY344864. $ represents significance compared to formoterol.

Pretreatment with KT5823 or skepinone decreases nuclear phosphorylated PGC-1α at serine and threonine residues in the presence of riociguat

Phosphorylation of PGC-1α at serine and threonine sites by p38 can increase the stability of PGC-1α, resulting in its translocation to the nucleus and transcription of PGC-1α. RPTC were pretreated with KT5823 for 30 min and then exposed to vehicle or riociguat for 2 h. RPTC were subjected to subcellular fractionation and tested for purity of nuclear and cytosolic fractions by measuring α-tubulin, a cytosolic marker, and Lamin B, a nuclear marker[7,11]. PGC-1α was immunoprecipitated from the nuclear and cytosolic fractions, and immunoblotted for phosphorylated serine and threonine residues (Figure 4A,C). Phosphorylated PGC-1α in the nuclear fraction was increased by 1.64-fold following riociguat treatment (Figure 4B), and decreased to control levels in the presence of KT5823. There were no changes in PGC-1α phosphorylation in the cytosolic fraction compared to vehicle control (Figure 4C-D).

RPTC were pretreated with skepinone for 30 min and then exposed to vehicle or riociguat for 2 h. Phosphorylated PGC-1α was measured in nuclear and cytosolic fractions. Skepinone alone had no effect on phosphorylated PGC-1α in the nucleus (Figure 5A,B). Skepinone decreased phosphorylated PGC-1α in the nucleus to control levels when exposed to riociguat. Phosphorylated PGC-1α did not change in the cytosolic fraction compared to vehicle control (Figure 5C,D).

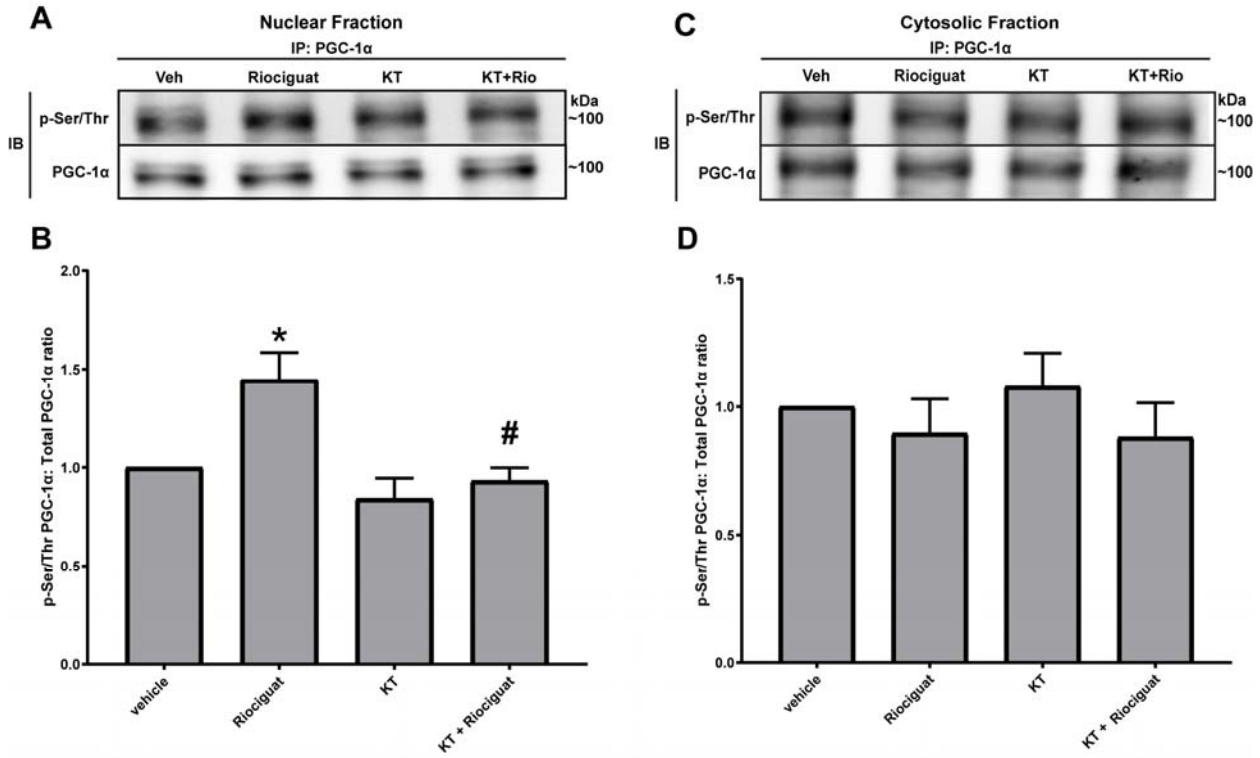

Figure 4: Pretreatment with KT5823 decreases nuclear phosphorylated PGC-1α in the presence of riociguat. A and C) Phosphorylated serine and threonine residues were measured following immunoprecipitation of PGC-1α by immunoblot analysis in nuclear and cytosol fractions after 30 min pretreatment with Vehicle or KT5823 (KT) followed by exposure to DMSO and riociguat for 2 hr. Total PGC-1α expression was measured after immunoprecipitation. B and D) Densitometry analysis for phosphorylated serine and threonine residue in the nuclear and cytosolic fractions. Data are represented as mean S.E., N=6. * represents significance compared to Vehicle control ($p<0.05$). # represents significance compared to riociguat.

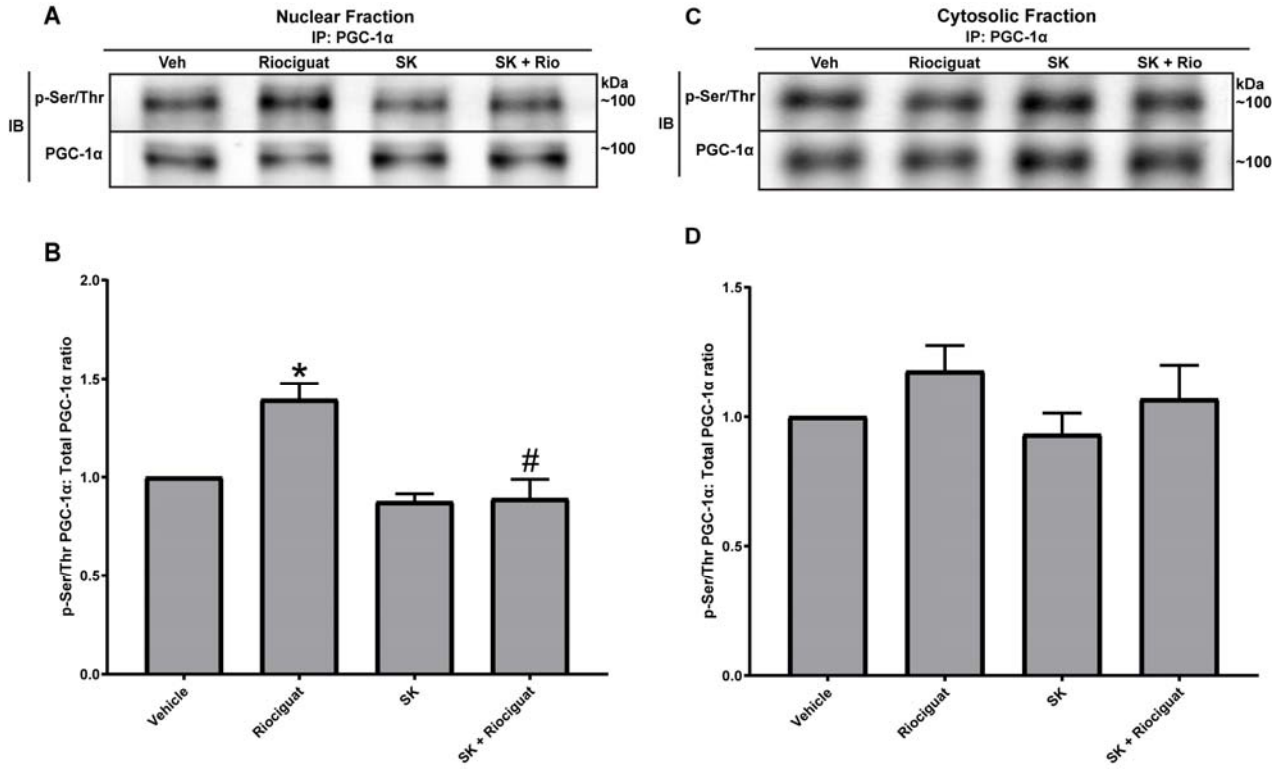

Figure 5: Pretreatment with skepinone decreases nuclear phosphorylated PGC-1α at serine and threonine sites in the nucleus

A and C) Phosphorylated serine and threonine residues were measured following immunoprecipitation of PGC-1α by immunoblot analysis after 30 min treatment with DMSO or 100nM SK followed by exposure to DMSO and riociguat for 2 hr, in cytosol and nuclear fractions. Total PGC-1α expression was measured after immunoprecipitation. B and D) Densitometry analysis for phosphorylated serine and threonine residues in the cytosol and nuclear fractions. Data are represented as mean S.E., N=6-7. * represents significance compared to Vehicle control ($p<0.05$). # represents significance compared to riociguat.

Skepinone decreases nuclear phosphorylated PGC-1α in the renal cortex

Based on the above cellular data, we determined if p38 inhibition alters phosphorylated PGC-1α in the kidney. We performed a dose response experiment using skepinone and measured p38 phosphorylation in the renal cortex. Naïve mice were injected with 1 mg/kg, 3 mg/kg, and 10mg/kg of skepinone and then euthanized 6 h after injection. At all three doses, skepinone equally blocked p38 phosphorylation by more than 50% (Figure 6A,B). Using the lowest dose of skepinone (1 mg/kg), the number of mice was increased (N=6-7) (Figure 6C) and skepinone decreased p38 phosphorylation by 75% (Figure 6D).

The next experiment measured phosphorylated PGC-1α in cytosolic and nuclear fractions of the renal cortex (Figure 6F and H). Mice were treated with skepinone (1 mg/kg) for 6 h and renal cortex was subcellular fractionated. The purity of cytosolic and nuclear fractions was tested (Figure 6E). In the cytosolic fraction, skepinone had no affect on phosphorylated PGC-1α; however, in the nuclear fraction, skepinone decreased phosphorylated PGC-1α by 50% (Figure 6G, I).

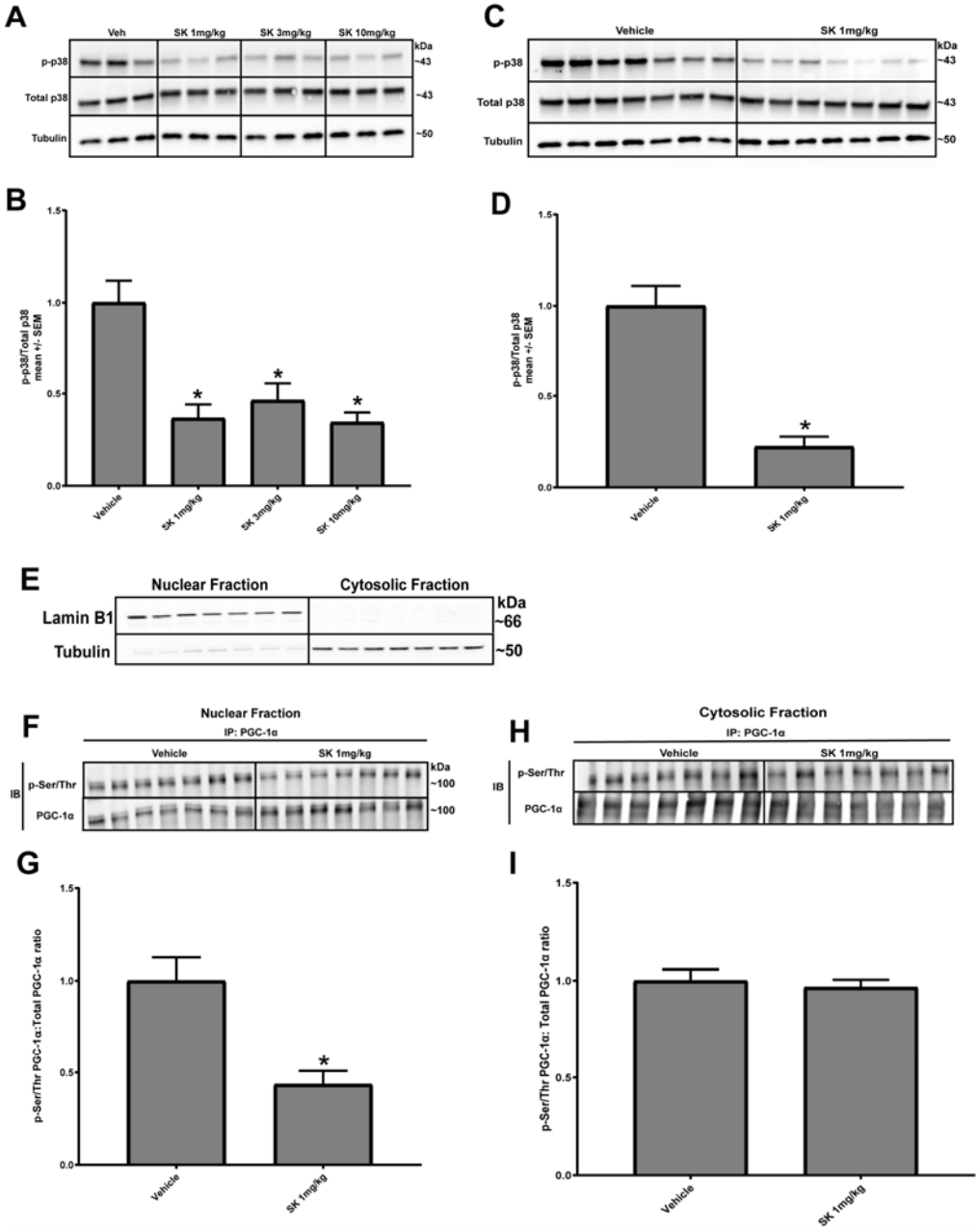

Figure 6: Skepinone (SK) decreases nuclear phosphorylated PGC-1α in the renal cortex
Representative blot for p-p38, total p38, and tubulin in naïve mice, 6 hr after treatment with 1 mg/kg, 3 mg/kg, 10 mg/kg of SK. C) Representative blot for p-p38, total p38, and tubulin with 1 mg/kg SK. B-D) Densitometry analysis for p38 protein. Data are represented as mean S.E., N=3-7. E) Representative blot for tubulin and lamin B1 in nuclear and cytosol fractions. F and H) Phosphorylated serine and threonine residues were measured following immunoprecipitation of PGC-1α in cytosol and nuclear fractions by immunoblot analysis. G and I) Densitometry analysis for phosphorylated serine and threonine residue in the cytosol and nuclear fractions. Data are represented as mean S.E., N=7 * represents significance compared to Vehicle ($p<0.05$). Black lines in the center of blots are used for dividing experimental groups only and do not alter information contained therein.

Discussion

Previous studies from our laboratory have shown that cGMP, not cAMP, induces MB in RPTC[31]. PDE3 inhibitors such as cilostamide and trequinsin, compounds that prevent the degradation of cGMP, also induce MB in RPTC[31]. *In vivo*, sildenafil, a PDE5 inhibitor, also induces MB in the renal cortex of naïve mice[31]. However, the mechanisms by which cGMP can induce MB are still under investigation for different cell types.

We showed the induction of MB in RPTC treated with formoterol, a β_2AR agonist, and LY344864, a 5-HT_{1F} agonist. Moreover, we reported that sGC and cGMP are important components for signaling MB in RPTC[4,10]. In this study, we proposed a signaling pathway between sGC and MB, sGC/cGMP/PKG/p38/PGC-1α in RTPC. In addition, we pharmacologically targeted sGC by administering riociguat, an sGC stimulator that targets the reduced/heme-dependent form[2,16,20,29].

To elucidate the role of p38 in the sGC-dependent induction of MB, skepinone, a potent and selective ATP-competitive inhibitor for p38α and p38β inhibitor, was used[17]. Previous studies have shown that p38 can directly phosphorylate PGC-1α at Threonine 298, Threonine 262, and Serine 265 in the cytosol, causing its translocation to the nucleus to sustain PGC-1α transcription and therefore MB[24]. We show that inhibition of PKG activation and p38 phosphorylation, decreases nuclear phosphorylated PGC-1α when RPTC are exposed to pharmacological compounds riociguat, formoterol and LY344864, demonstrating that PKG activation and p38 are needed in the pathway from sGC to MB. Further support for this pathway is that administration of skepinone *in vivo,* decreased nuclear phosphorylated PGC-1α in the renal cortex.

Previous literature shows that PKG activation can lead to p38 phosphorylation and that p38 is a downstream associated target of PKG[1,3,18,26]. Based on this literature, we did not explore the effect of skepinone on PKG activation in the presence of riociguat. Although the literature provides evidence for other downstream effectors such as ERK1/2, GSK3β, and Akt, we chose to focus on p38 for its role in NO signaling, cGMP/PKG dependent signaling, and regulation of PGC-1α[3,8,18,26,27].

In summary, we have elucidated a pathway for sGC-dependent induction of MB by investigating the importance of PKG and subsequent activation of p38 leading to an increase in nuclear phosphorylated PGC-1α by pharmacological compounds. This study supports our previous work with potent inducers of MB and show the importance of sGC/cGMP in the signaling pathways leading to the induction of MB in the kidney.

1 Bordicchia, M. *et al.* Cardiac natriuretic peptides act via p38 MAPK to induce the brown fat thermogenic program in mouse and human adipocytes. *J Clin Invest* **122**, 1022-1036, doi:10.1172/jci59701 (2012).

2 Breitenstein, S., Roessig, L., Sandner, P. & Lewis, K. S. Novel sGC Stimulators and sGC Activators for the Treatment of Heart Failure. *Handb. Exp. Pharmacol.* **243**, 225-247, doi:10.1007/164_2016_100 (2017).

3 Browning, D. D., McShane, M. P., Marty, C. & Ye, R. D. Nitric oxide activation of p38 mitogen-activated protein kinase in 293T fibroblasts requires cGMP-dependent protein kinase. *J Biol Chem* **275**, 2811-2816 (2000).

4 Cameron, R. B., Peterson, Y. K., Beeson, C. C. & Schnellmann, R. G. Structural and pharmacological basis for the induction of mitochondrial biogenesis by formoterol but not clenbuterol. *Sci. Rep.* **7**, 10578, doi:10.1038/s41598-017-11030-5 (2017).

5 Collins, S. A heart-adipose tissue connection in the regulation of energy metabolism. *Nat. Rev. Endocrinol.* **10**, 157-163, doi:10.1038/nrendo.2013.234 (2014).

6 Cook, A. L. & Haynes, J. M. Phosphorylation of the PKG substrate, vasodilator-stimulated phosphoprotein (VASP), in human cultured prostatic stromal cells. *Nitric Oxide* **16**, 10-17, doi:10.1016/j.niox.2006.09.003 (2007).

7 Dechat, T. *et al.* Nuclear lamins: major factors in the structural organization and function of the nucleus and chromatin. *Genes Dev.* **22**, 832-853, doi:10.1101/gad.1652708 (2008).

8 Fernandez-Marcos, P. J. & Auwerx, J. Regulation of PGC-1alpha, a nodal regulator of mitochondrial biogenesis. *Am. J. Clin. Nutr.* **93**, 884S-890, doi:10.3945/ajcn.110.001917 (2011).

9 Francis, S. H., Busch, J. L., Corbin, J. D. & Sibley, D. cGMP-dependent protein kinases and cGMP phosphodiesterases in nitric oxide and cGMP action. *Pharmacol. Rev.* **62**, 525-563, doi:10.1124/pr.110.002907 (2010).

10 Gibbs, W. S., Garrett, S. M., Beeson, C. C. & Schnellmann, R. G. Identification of dual mechanisms mediating 5-hydroxytryptamine receptor 1F-induced mitochondrial biogenesis. *Am. J. Physiol. Renal Physiol.* **314**, F260-f268, doi:10.1152/ajprenal.00324.2017 (2018).

11 Goldman, R. D., Gruenbaum, Y., Moir, R. D., Shumaker, D. K. & Spann, T. P. Nuclear lamins: building blocks of nuclear architecture. *Genes Dev.* **16**, 533-547, doi:10.1101/gad.960502 (2002).

12 Haas, B. *et al.* Protein kinase G controls brown fat cell differentiation and mitochondrial biogenesis. *Sci Signal* **2**, ra78, doi:10.1126/scisignal.2000511 (2009).

13 Harms, M. & Seale, P. Brown and beige fat: development, function and therapeutic potential. *Nat. Med.* **19**, 1252-1263, doi:10.1038/nm.3361 (2013).

14 Hofmann, F. The biology of cyclic GMP-dependent protein kinases. *J. Biol. Chem.* **280**, 1-4, doi:10.1074/jbc.R400035200 (2005).

15 Jornayvaz, F. R. & Shulman, G. I. Regulation of mitochondrial biogenesis. *Essays Biochem.* **47**, 69-84, doi:10.1042/bse0470069 (2010).

16 Khaybullina, D., Patel, A. & Zerilli, T. Riociguat (adempas): a novel agent for the treatment of pulmonary arterial hypertension and chronic thromboembolic pulmonary hypertension. *P & T : a peer-reviewed journal for formulary management* **39**, 749-758 (2014).

17 Koeberle, S. C. *et al.* Skepinone-L is a selective p38 mitogen-activated protein kinase inhibitor. *Nat. Chem. Biol.* **8**, 141-143, doi:10.1038/nchembio.761 (2011).
18 Li, Z., Zhang, G., Feil, R., Han, J. & Du, X. Sequential activation of p38 and ERK pathways by cGMP-dependent protein kinase leading to activation of the platelet integrin alphaIIb beta3. *Blood* **107**, 965-972, doi:10.1182/blood-2005-03-1308 (2006).
19 Maimaitiyiming, H. *et al.* Increasing cGMP-dependent protein kinase I activity attenuates cisplatin-induced kidney injury through protection of mitochondria function. *Am. J. Physiol. Renal Physiol.* **305**, F881-890, doi:10.1152/ajprenal.00192.2013 (2013).
20 Mitrovic, V., Jovanovic, A. & Lehinant, S. Soluble guanylate cyclase modulators in heart failure. *Curr. Heart Fail. Rep.* **8**, 38-44, doi:10.1007/s11897-010-0045-1 (2011).
21 Nisoli, E. *et al.* Mitochondrial biogenesis in mammals: the role of endogenous nitric oxide. *Science* **299**, 896-899, doi:10.1126/science.1079368 (2003).
22 Nisoli, E. *et al.* Mitochondrial biogenesis by NO yields functionally active mitochondria in mammals. *Proc. Natl. Acad. Sci. U. S. A.* **101**, 16507-16512, doi:10.1073/pnas.0405432101 (2004).
23 Nowak, G. & Schnellmann, R. G. L-ascorbic acid regulates growth and metabolism of renal cells: improvements in cell culture. *Am. J. Physiol.* **271**, C2072-2080, doi:10.1152/ajpcell.1996.271.6.C2072 (1996).
24 Puigserver, P. *et al.* Cytokine stimulation of energy expenditure through p38 MAP kinase activation of PPARgamma coactivator-1. *Mol. Cell* **8**, 971-982 (2001).
25 Puigserver, P. *et al.* A cold-inducible coactivator of nuclear receptors linked to adaptive thermogenesis. *Cell* **92**, 829-839, doi:10.1016/s0092-8674(00)81410-5 (1998).
26 Rabkin, S. W., Klassen, S. S. & Tsang, M. Y. Sodium nitroprusside activates p38 mitogen activated protein kinase through a cGMP/PKG independent mechanism. *Life Sci.* **81**, 640-646, doi:10.1016/j.lfs.2007.06.022 (2007).
27 Rasbach, K. A. & Schnellmann, R. G. Signaling of mitochondrial biogenesis following oxidant injury. *J. Biol. Chem.* **282**, 2355-2362, doi:10.1074/jbc.M608009200 (2007).
28 Shen, W. *et al.* Lipoamide or lipoic acid stimulates mitochondrial biogenesis in 3T3-L1 adipocytes via the endothelial NO synthase-cGMP-protein kinase G signalling pathway. *Br. J. Pharmacol.* **162**, 1213-1224, doi:10.1111/j.1476-5381.2010.01134.x (2011).
29 Stasch, J. P., Schlossmann, J. & Hocher, B. Renal effects of soluble guanylate cyclase stimulators and activators: a review of the preclinical evidence. *Curr. Opin. Pharmacol.* **21**, 95-104, doi:10.1016/j.coph.2014.12.014 (2015).
30 Tedesco, L. *et al.* Cannabinoid type 1 receptor blockade promotes mitochondrial biogenesis through endothelial nitric oxide synthase expression in white adipocytes. *Diabetes* **57**, 2028-2036, doi:10.2337/db07-1623 (2008).
31 Whitaker, R. M., Wills, L. P., Stallons, L. J. & Schnellmann, R. G. cGMP-selective phosphodiesterase inhibitors stimulate mitochondrial biogenesis and promote recovery from acute kidney injury. *J Pharmacol Exp Ther* **347**, 626-634, doi:10.1124/jpet.113.208017 (2013).